

Tensile strength of liquid ^4He

J. A. Nissen,* E. Bodegom, L. C. Brodie, and J. S. Semura

Department of Physics and Environmental Sciences and Resources Program, Portland State University, Portland, Oregon 97207

(Received 23 January 1989; revised manuscript received 19 June 1989)

Experiments to measure the tensile strength of liquids have often failed to reach the predicted value, presumably due to the onset of heterogeneous nucleation. Since it seemed impossible to completely eliminate all heterogeneous nucleation, we adopted a strategy that minimized its effect. A piezoelectric transducer in the form of a hemispherical shell was used to focus a short burst of ultrasound into a small volume of liquid ^4He . The onset of cavitation was detected by the scattering of laser light. The experimental results both above and below the λ transition are in agreement with homogeneous-nucleation theory for a nucleation rate of approximately 10^{15} critical-size bubbles/s cm^3 . An apparent lowering of the tensile strength near the extension of the λ line into the metastable liquid is noted and discussed. This experiment extends the range of confirmation of the theoretically predicted tensile strength of liquids to a reduced pressure eight times further into the negative-pressure region than previous studies in any other liquid.

I. INTRODUCTION

It is well known that most liquids exhibit a tensile strength which is much smaller in magnitude than the tensile strength predicted by homogeneous nucleation theory. In fact, in only three liquids has the theoretical tensile strength ever been reached. The tensile limits in ether and *n*-hexane have been reached by Apfel¹ and that of helium II by this laboratory.² This lack of agreement for most liquids is often attributed to the difficulty of preparing liquid samples free from inclusions of foreign gases which freely expand when the host liquid is brought into the metastable region, thus reducing the ability of the liquid to sustain the tensile stress. Liquid helium occupies a unique place among liquids for tensile strength measurements in this regard. Helium is a liquid only at temperatures colder than 5.2 K, so that all foreign gases are frozen out of the helium and are therefore unavailable as gas pockets which act to lower the tensile strength. Furthermore, due to the excellent wetting properties of liquid helium (helium should have a near zero contact angle with all solids), metastable pockets of helium vapor residing on surfaces last only a few seconds under saturated vapor pressure conditions and are therefore generally unavailable as heterogeneous nucleation sites.³ The situation is even more advantageous in superfluid helium, which has the ability to flow into minute channels and fill any cracks or pits, thus quickly eliminating them as sites for nucleation due to trapped vapor. Despite these advantages, the results of previous investigators over the past 30 years have been in stark disagreement with the theoretical tensile strength of ^4He .⁴⁻²³

Recent theoretical developments, however, cast doubt upon the hypothesis that heterogeneous nucleation will be absent for a substance, such as liquid helium, which perfectly wets solid substrates. Thormählen has calculated that for deeply undercut surface irregularities it is energetically favorable to create vapor cavities at the solid

surface even for liquids with a zero contact angle.²⁴ The historic difficulty in reaching the theoretical tensile strength in both helium I and helium II supports this result. It appears then that the absence of trapped vapor pockets is not in itself sufficient to prevent the solid surface from weakening the liquid, and so an experimental method which is capable of reaching the theoretical tensile strength despite the presence of heterogeneous nucleation must be used.

For very rapid pressure excursions, the liquid can be carried far into the metastable region despite the presence of steady-state heterogeneous nucleation. This is possible because the potential number of precritical nuclei available for homogeneous nucleation far outweighs the potential number of sites available for heterogeneous nucleation. The pressure excursion must be rapid to ensure that a thermodynamic state deep in the metastable region of the liquid is reached before bubble growth at heterogeneous nucleation sites has time to appreciably alter the flow of energy into the liquid. This principle pioneered by Skripov²⁵ has been used effectively in the past to reach the limit of superheat (which is also predicted by homogeneous nucleation theory) for many liquids including liquid helium.²⁶⁻²⁸

In this paper we report new measurements of the tensile strength of liquid helium. The cavitation limit was reached by focusing a short burst of ultrasound into a small volume of helium and detecting the onset of cavitation by the scattering of laser light. Over most of the temperature range investigated our data agree well with the homogeneous nucleation theory, thus verifying the theory over a range of reduced pressures almost an order of magnitude larger than previous studies in any other liquid.

Section II gives the details of the equipment and Sec. III describes the procedure. The visual observations of the cavitation zone are given in Sec. IV. A description of temperature corrections follows. Section VI gives the ex-

perimental results and compares them with nucleation theory. The entire paper is summarized in Sec. VII.

II. APPARATUS

Short bursts of ultrasound were focused in liquid helium by a piezoelectric transducer formed in the shape of a hemispherical shell. The transducer, made from Channel 5400 Navy I piezoelectric material, has an inside radius of 0.625 cm and an outside radius of 1.043 cm. It was operated in its thickness mode at the half-wave resonant frequency of 566 kHz. The transducer was mounted with its concave side facing up in order to prevent vapor bubbles from collecting on the inner surface of the transducer in helium I. These bubbles were continually formed at the Dewar walls and at the transducer during application of power. The transducer was supported on the outer hemispherical surface at two points by Teflon and at a third point by a gold electrical contact. Electrical connections were made with fine magnet wire soldered to the electrodes of the piezoelectric ceramic. Care was taken to minimize acoustic radiation into the connections and supporting structure. Two grooves were cut radially into the rim so that the focal zone, which lies half below the rim, would be visible from the side (Fig. 1).

The driving signal to the piezoelectric transducer was obtained from a function generator which was gated on and off with a gate pulse typically 1 ms in duration. The gated sinusoidal signal was amplified to provide up to 20 W of power, followed by a step-up transformer to provide impedance matching between the power amplifier and the piezoelectric transducer.

The helium bath pressure was monitored with an accuracy of ± 0.3 mbar by a capacitive pressure gauge. The bath temperature was determined to within ± 10 mK by a germanium thermometer which was calibrated against the bath pressure and mounted at the same level as the cavitation zone. With this arrangement the temperature

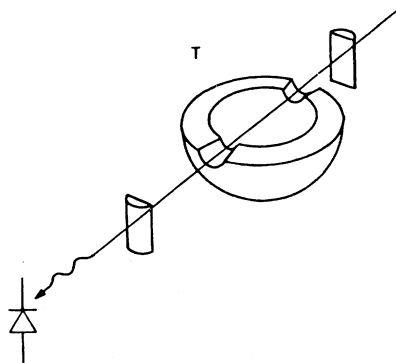


FIG. 1. Setup to observe the cavitation zone and measure the pressure amplitude. A cylindrical lens was used to focus laser light on the acoustic focal zone of piezoelectrical transducer T. After being recollimated by a second cylindrical lens, the light intensity of the zeroth diffraction order is monitored by a photodiode.

could be monitored while the bath was slightly overpressurized.

The experiment was conducted in a 1.5-l Dewar with transverse optical windows allowing the use of laser light to probe the cavitation zone, that is, the focal zone of the hemispherical transducer. The transmitted light intensity was monitored with a photodiode configured to respond to signals with rise times shorter than a microsecond. The He-Ne laser was chosen to detect the onset of nucleation for three reasons. First, the light probe has precise spatial resolution, enabling the discrimination between cavitation on the transducer's surface and at the transducer's focus. Second, the laser light can be used as a pressure transducer via the acousto-optic interaction.²⁹ Third, laser scattering is more sensitive to small bubbles than sonic detection, a method which previously was often employed to detect cavitation. Neither method is capable of detecting 2-nm bubbles, the critical radius for observable nucleation rates. However, the scattering cross section for light from bubbles smaller than the wavelength of light is proportional to the number density of bubbles,³⁰ which is large under the conditions of intense nucleation in the cavitation zone in this experiment. The result is that by the time the bubbles have grown to approximately 100 nm, the light that is scattered out of the laser beam can be detected with a photomultiplier. Even at these relatively large bubble sizes acoustic detection is extremely difficult because the resonant frequency is high [on the order of 100 MHz (Ref. 31)].

III. EXPERIMENTAL METHODS

Two separate methods, which have been discussed in detail elsewhere,^{2,32,33} were used to determine the acoustic pressure amplitude at the focus of the piezoelectric transducer. In the first method, the electrical power consumed by the transducer tuned to its series resonance is related to the acoustic power radiated into the liquid through an equivalent piezoelectric circuit.³⁴ The pressure amplitude at the focus was then calculated from the radiated power, the geometry of the transducer, and the nonlinear absorption of sound due to shock waves.³⁵ The experimental error in measuring the pressure amplitude by this method is estimated to be less than 10%.

In the second method, the acousto-optic interaction was used to measure the pressure amplitude at the focal plane of the piezoelectric transducer. Pressure variations in the liquid cause periodic variations in the index of refraction, creating an optical phase grating. When light is incident at right angles to the propagation vector of the sound, the intensity of the n th order diffracted light can be calculated by the Raman-Nath theory in the case of plane ultrasonic waves. It can be shown that this intensity is proportional to the square of the n th-order Bessel function of the Raman-Nath parameter. This parameter is linearly related to the pressure amplitude. In the case of a profiled sound beam, as we have here, modifications to the Raman-Nath theory are required.^{32,33} The light intensity of each diffraction order, however, can still be related to the acoustic pressure amplitude. Figure 2 is

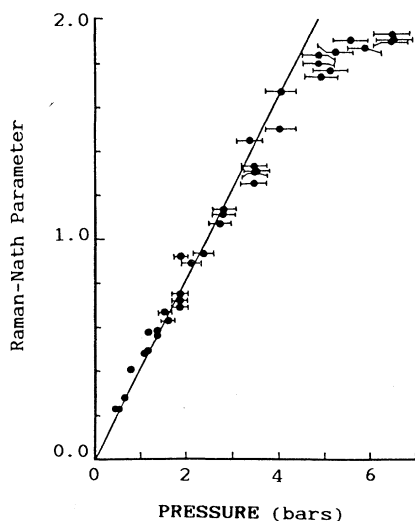


FIG. 2. The Raman-Nath parameter as a function of the applied pressure in liquid helium at 1.9 K. The solid line represents calculations using the modified Raman-Nath theory. The ordinates of the data points are obtained from the light intensities, and the abscissas are obtained from the acoustic power method. The discrepancy at large amplitudes can be resolved by taking into account higher harmonics of the sound wave.

used to show that data calculated with the modified theory are consistent with the pressure amplitudes derived from the acoustic power method. The Raman-Nath parameter is plotted as a function of the pressure amplitude at the focal point calculated from the acoustic power transmitted into liquid helium. The Raman-Nath parameter was obtained from measurements of the light intensities. These data were taken using the apparatus which was subsequently employed in the tensile strength measurements. The error bars in the graph indicate the uncertainty with which the pressure is known in the acoustic method; the uncertainty in the Raman-Nath parameter is too small to be indicated in the figure. The data agree well with the theoretical calculation of the Raman-Nath parameter up to a pressure amplitude of 4 bars. The discrepancy at higher acoustic pressures is due to the assumption that the acoustic wave is purely sinusoidal. At higher-pressure amplitudes a shock wave develops and the discrepancy can be resolved by taking into account the light diffracted by the higher harmonics of the acoustic wave.

A typical sequence of experiments for determining the tensile strength is presented in Fig. 3. The oscilloscope traces show the output of the photodiode, which detected the zeroth order of the laser light diffracted from the cavitation zone. In the upper trace, the piezoelectric transducer was gated on at time zero. In 40 μs , the sound reached the focal point of the transducer and the light intensity dropped as light was diffracted from the beam. For the next 0.4 ms, while the output of the piezoelectric transducer built to a steady state, the amplitude of the acoustic wave at the focus increased, after which there

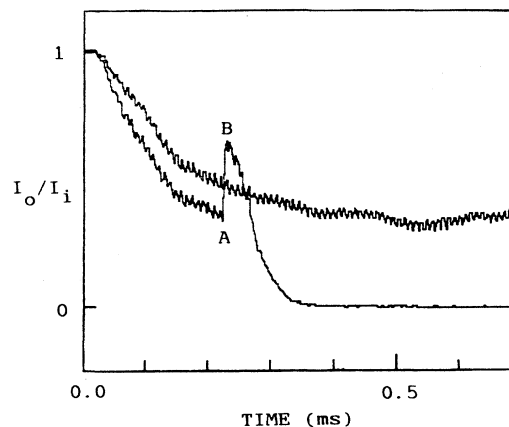


FIG. 3. Oscilloscope traces of the output of the photodiode monitoring the laser beam. The piezoelectric transducer was gated on at $t=0$. After 40 μs , the acoustic wave reached the focal zone, diffracting the incident light out of the zeroth order. This reduced the intensity at the photodiode I_0 below the incident intensity I_i . As the pressure amplitude increased, more light was diffracted from the zeroth order. If the acoustic pressure amplitude reached a critical value, a strong signal due to cavitation was observed. At point *A*, bubble nucleation began absorbing energy away from the acoustic wave, reducing the pressure amplitude at the focus and allowing more light to fall on the photodiode placed at the zeroth order. At point *B*, the nucleated bubbles has grown large enough to scatter the laser light and the light reaching the photodiode dropped to undetectable levels.

was no change in the light intensity. For the lower trace, the driving voltage of the piezoelectric transducer was slightly increased. More light was diffracted from the beam, and a characteristic signal appeared at 0.2 ms due to cavitation.

Measurements of the acoustic power radiated into the liquid and of the light intensity diffracted by the ultrasound were made between 1.6 and 4.2 K, allowing several seconds to elapse between gate pulses to prevent warming of the bath and the transducer. The power to each successive gated signal was increased until the characteristic cavitation signal was observed between 0.2 and 0.5 ms from the start of the sound burst. If the delay time to the onset of cavitation was shorter than 0.2 ms, the output of the transducer had not reached the steady state and therefore the power radiated into the liquid could not be accurately calculated. Below the λ point, if the delay time was greater than 0.5 ms, there was the possibility that focused second sound emanating from the transducer would arrive at the cavitation zone (the speed of second sound is less than one-tenth the speed of first sound between 1.6 and 2.17 K), thus increasing the uncertainty of the liquid temperature.

At bath temperatures above 3 K, the calculation of the focal pressure from the radiated power method and the diffraction of light method were in serious disagreement. This was because at warmer bath temperatures the inter-

nal losses in the transducer were enough to cause vapor nucleation on the surface of the transducer due to the superheating of the liquid. Power was therefore lost from the acoustic radiation to the growing bubbles and additionally the liquid was acoustically decoupled from the transducer, which led to an unrealistically high calculation of the pressure amplitude at the focus. The problem of superheating by ultrasonic transducers in liquid helium is further exacerbated by an effect recently observed by Bodegom *et al.* in which the nucleation rate at the surface of a heater thermometer was dramatically enhanced by low levels of ultrasound.³⁶ The light diffraction method of calculating the pressure amplitude at the focus was unaffected by nucleation near the surface of the piezoelectric transducer, and for this reason the acousto-optic method of pressure measurement was adopted for tensile-strength measurements in helium I.

IV. VISUAL OBSERVATIONS

By visual observations, it was easily verified that light was being scattered from the focal zone of the piezoelectric transducer at the same pressure amplitudes at which cavitation was observed with the photodiode. The light scattering was visible for a fraction of a second even with a gate width of 0.5 ms. Using a spread beam and a lens, an image of the focal zone could be projected onto a screen. A dark plume was visible whenever the pressure amplitude was the same as that at which cavitation was observed with the photodiode. In helium I, the dark plume could be seen for only an instant before it was washed out by clouds of bubbles emanating from the transducer surface. These later bubbles were caused by the superheating of a thin layer of helium at the surface of the transducer as the transducer warmed due to internal losses.

High-speed photographs of the cavitation zone revealed that the cavitation and plume were fully developed within 0.5 ms of the inception of nucleation and that the cavitation was occurring at the focus of the transducer. The plume, which was 0.14 cm long, cannot be accounted for by the buoyancy of the bubbles, since in 0.5 ms the buoyant force would move the bubbles an insignificant distance. It was therefore surmised that radiation pressure on the bubbles resulted in an acoustic streaming of the helium within this time interval.

V. TEMPERATURE CORRECTIONS

The pressure amplitude of the acoustic wave in the cavitation zone can be calculated from the acoustic power radiated into the liquid or from the diffraction of light from the sound field; but in order to compare the results of the experimentally derived tensile strength with homogeneous nucleation theory, it is first necessary to determine the temperature change that accompanies the pressure change. If no shock wave is present, then the compression and rarefaction of the wave takes place adiabatically. The temperature change can be estimated from the thermodynamic relation

$$TdS=0=C_p dT-TV\alpha_p dP, \quad (1)$$

where C_p is the specific-heat capacity at constant pressure, V is the specific volume, and α_p is the volume expansivity at constant pressure. Equation (1) can be integrated to find the temperature change if C_p and α_p are known as functions of P and T . Unfortunately, very few thermodynamic data are available for the metastable region in liquid helium. In order to obtain the best estimate of the temperature change, C_p and α_p were extrapolated into the metastable liquid from the values in the stable liquid region;³² nearly the same result is obtained by using the saturation values of the heat capacity and expansivity at the bath temperature. The temperature change was estimated from Eq. (1) for each data point above the λ line. The change in temperature from the bath temperature was found to be at most -0.4 K for the negative-pressure excursions in this experiment.

Close to the λ line, the value of the heat capacity diverges. As a result, the adiabatic temperature change becomes vanishingly small as the λ line is approached. Below the λ line, α_p is negative; therefore helium II warms upon expansion and cools upon compression. The pressure excursion is, however, approximately isothermal due to the very small value of α_p in this region. Therefore we expect no significant error to be introduced if the expansion in helium II is considered to take place isothermally in the temperature range of this experiment.

When shock waves are present in the liquid helium, additional heating due to the absorption of acoustic energy must be considered. To estimate the magnitude of the heating, it is sufficient to examine the effect of shock waves at 1.6 K, at which temperature the acoustic amplitude is the greatest and the value of the heat capacity is the smallest. Following Rozenberg,³⁷ the shock wave is formed at a distance r_1 from the focus given by the equation

$$r_1=r_0 \exp(-1/\sigma_0), \quad (2)$$

where r_0 is the radius of curvature of the transducer and σ_0 is given by the expression

$$\sigma_0=\epsilon k r_0 (P_0/\rho c_0^2), \quad (3)$$

where k is the acoustic wave number, $2\pi/\lambda$, P_0 is the pressure amplitude at the surface of the transducer, and c_0 is the speed of sound in the unperturbed medium of density ρ . The parameter ϵ is related to the nonlinearity parameter B/A by the expression $\epsilon=\frac{1}{2}(B/A)+1$ and ranges from 3.5 to 4.0 along the coexistence curve.^{32,38}

The attenuation of the acoustic wave occurs within a hemisphere of radius r_1 . If it is assumed that the energy is absorbed uniformly by the mass of helium m within this hemisphere, then the temperature rise ΔT is given by

$$\Delta T=\Delta E/mC_p=25 mK, \quad (4)$$

where ΔE is the acoustic energy absorbed by the helium during the period of shock-wave production, here taken to be approximately 0.2 ms. The energy absorbed, ΔE , is the difference between the acoustic energy radiated from the transducer and the acoustic energy arriving at the focal plane. The temperature change due to the absorption of sound is thus seen to be negligible at bath temperatures

above 1.6 K.

VI. COMPARISON WITH HOMOGENEOUS NUCLEATION THEORY

In reality the tensile strength of a liquid is not a single value but can be viewed more clearly as a family of curves described by homogeneous nucleation theories for liquid-to-vapor phase transitions.^{39,40} These theories calculate the rate of bubble formation and apply equally to situations in which, for example, the liquid is brought into its metastable region by stretching the liquid at constant temperature, by superheating at constant positive pressure, or a combination of the two methods. The rate of bubble formation is calculated by considering the minimum work that must be done to form a vapor bubble in the liquid. This work of formation constitutes an activation-energy barrier to the formation of bubbles by thermodynamic fluctuations in the liquid. If random fluctuations produce a cavity with a radius smaller than r_c , the critical radius, which corresponds to the maximum in the work of formation, the bubble will tend to spontaneously collapse. If, on the other hand, the random fluctuations lead to the formation of a bubble with a radius larger than r_c , the bubble can only decrease its energy by growing. The further the excursion into the metastable region, the lower the height of the free-energy barrier; therefore, the probability per unit time that a bubble will be formed with a radius greater than r_c will be greatly increased.

The rate of formation of bubbles per unit volume in steady state J can be calculated from nucleation theory, where the rate expression takes the usual activation energy form:

$$J \propto \exp(-W_c/kT), \quad (5)$$

where k is Boltzmann's constant, T the temperature, and W_c the work necessary to form a bubble with radius r_c . Blander and Katz⁴⁰ write the rate equation explicitly as

$$J = N \left[\frac{2\sigma}{\pi m B} \right]^{1/2} \exp \left[\frac{-16\pi\sigma^3}{3kT(P_V - P_L)^2} \right], \quad (6)$$

where N is the particle number density of the liquid, m is the molecular mass, σ is the surface tension, and B is a factor which is approximately 1 for cavitation and $\frac{2}{3}$ for superheating. In the laboratory the equilibrium vapor pressure P_e is the quantity that is directly measured, rather than P_V , the vapor pressure inside the bubble. Therefore, it is convenient to introduce the Poynting correction δ relating P_e to P_V

$$P_V - P_L \cong (P_e - P_L)\delta. \quad (7)$$

The Poynting correction δ can be expressed as

$$\delta = 1 - \rho_V/\rho_L + \frac{1}{2}(\rho_V/\rho_L)^2, \quad (8)$$

where ρ_V and ρ_L are, respectively, the vapor and liquid densities. ρ_V/ρ_L is about 0.1 at 4 K and decreases rapidly with temperature.

Figure 4 displays three theoretical curves based on Eqs. (6) and (8) for homogeneous nucleation in ^4He . The change to the more recent surface tension data of Iino⁴¹ has eliminated a slight bump near the λ temperature which resulted from the use of smoothed data to calculate previously published homogeneous nucleation curves.^{2,31,32,42} One notable feature of this graph is that even a small pressure or temperature change makes an

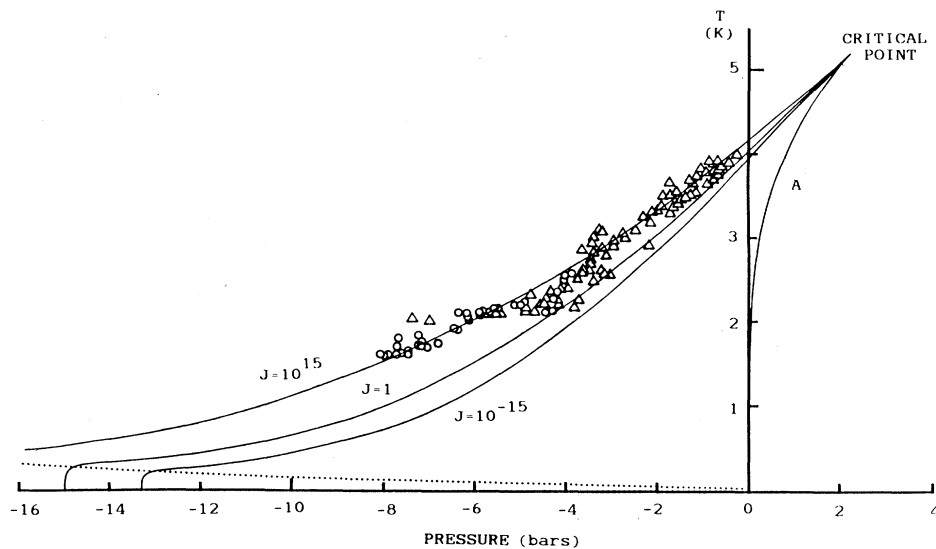


FIG. 4. The theoretical nucleation curves for three nucleation rates. The curves for $J=1$ and $J=10^{-15}$ critical-size nuclei are included for comparison. The experimental data are consistent with a nucleation rate of $J=10^{15}$ critical-size nuclei/s cm^3 . Data represented by the open circles were obtained from considerations of the focused acoustic power, while data represented by the triangles were obtained from the diffraction of light due to the acoustic waves. The statistical nature of nucleation is apparent from the scatter of the data. Curve A is the coexistence curve and the dotted line represents the expected limit of quantum nucleation.

enormous change in the nucleation rate. Above 4 K, the rate of bubble formation per cm^3 varies from $J=10^{-15}$ bubbles/s (one bubble every 30 million years on the average) to $J=10^{15}$ bubbles formed every second, within a pressure change of a few tenths of a bar. The other notable feature is that at temperatures below approximately 0.5 K the nucleation theories so far discussed are no longer sufficient to describe the fluctuations. At these lower temperatures, quantum fluctuations are expected to predominate over thermal fluctuations and the nucleation rate should tend to become temperature independent.^{42,43}

The results of the pressure measurements corrected for the adiabatic temperature change are graphed in Fig. 4. The data are in agreement with Becker-Döring theory for $J=10^{15}$ critical nuclei/s cm^3 over most of the temperature range. To see if this is reasonable, a rough estimate can be made of the rate that would be necessary to create one critical nucleus in the cavitation zone in one negative-pressure excursion. For an aperture angle of 90° , the radius of the acoustic focal zone of the transducer (i.e., the Airy disk) is π/k , where k is the wave number. The volume used in this experiment was approximately 10^{-5} cm^3 . In each pressure excursion cycle, the liquid was exposed to large negative pressures for a fraction of a microsecond. Therefore, to have a high probability of producing one bubble, J must be on the order of 10^{12} critical-size bubbles/s cm^3 . This is the minimum rate for homogeneous nucleation consistent with the experimental conditions.

More information on the nucleation rate is available from the diffracted light. An examination of the diffracted light intensity shown in Fig. 3 reveals that the moment nucleation begins (point *A*), there is a dramatic increase in the intensity of the zeroth diffraction order. Immediately after nucleation begins, the bubbles are too small to scatter the light, but they are absorbing power from the acoustic wave as they grow. The absorption of power manifests itself as a decrease in the acoustic pressure amplitude, causing an increase in the zeroth-order light intensity. About $10 \mu\text{s}$ after the start of nucleation, the light reaching the photodiode reaches a sharp maximum (point *B*) and subsequently decreases to undetectable levels. The sharp maximum at point *B* is coincident with the appearance of light scattered from microscopic bubbles produced in the cavitation zone. At the sharp peak in the photodiode output, the bubbles have grown large enough to scatter the laser beam, after which the light intensity decreases again.

The total energy absorbed from the ultrasound during the time interval from the inception of nucleation to the beginning of significant light scattering can be estimated from the light-intensity curve. The energy absorbed from the ultrasound during the interval from *A* to *B* is on the order of 4 erg. The energy U stored in a bubble of radius r is taken to be given by

$$U = 4\pi r^2 \sigma + (P_V - P_L) \frac{4}{3} \pi r^3. \quad (9)$$

At point *B* the average bubble radius is on the order of the wavelength of the He-Ne laser light and $P_V - P_L$ is on the order of 3 bars. The energy stored in the average bubble is therefore on the order of 10^{-7} erg. An estimate

of the nucleation rate can now be made based on the absorbed energy, the volume of the cavitation zone, and the time available for bubble formation. The result of this calculation (making the rather extreme assumption that all the critical size nuclei are formed in the first $0.1 \mu\text{s}$) is a nucleation rate of $J=10^{19}$ critical-size nuclei/s cm^3 . Since part of the absorbed energy is reemitted from oscillating bubbles as random acoustic radiation and part is used in acoustic streaming and heating of the cavitation zone, this estimate should be considered an upper limit to the nucleation rate. Moreover, the shock waves emitted from oscillating bubbles may enhance the nucleation rate once nucleation begins.

Thus a value of $J=10^{15}$ critical-size nuclei/s cm^3 as is indicated by our data, appears to be reasonable, since it lies between the two extremes of $J=10^{12}$ and $J=10^{19}$ critical-size nuclei/s cm^3 .

As an aside, it is interesting to note that an estimate of the average rate of bubble growth can be obtained from the time delay between the inception of nucleation and the scattering of light from the bubbles. The bubbles grow to approximately 100 nm in six acoustic cycles and only grow during the negative-pressure portion of the cycle. This provides the estimate of the average radial growth rate on the order of 1 cm/s.

Special consideration must be given to the tensile strength near the λ transition. It is seen from Fig. 4 that the tensile strength is lowered to the value one would expect for a nucleation rate of approximately 1 critical nucleus/s cm^3 . This rate is in disagreement with the experimental conditions. One may try to explain this discrepancy by a systematic error in calculating the pressure and the temperature in the focal zone of the transducer, since many of the physical properties such as the speed of sound and the heat capacity are changing very rapidly near the λ transition. However, the agreement between the two methods of determining the pressure amplitude, which have differing functional dependence on these physical properties, lends credence to the effect being physical rather than an artifact of the calculations.

Of the possible mechanisms for heterogeneous nucleation that could account for this discrepancy, the often cited hypothesis of bubble nucleation on quantized vortices deserves special attention since it is likely to be sensitive to presence of the λ transition. While the decay of a vortex ring from quantum number $n=1$ to $n=0$ could release enough energy into the volume of a critical-size bubble to account for the enhanced nucleation rate observed in this experiment,³² much of the evidence of vapor nucleation on quantized vortices must be reassessed in view of more recent data indicating that acoustic radiation from quantized vortices may have been mistakenly identified as cavitation noise.⁴⁴ Furthermore, the enhancement of the nucleation rate observed in this experiment occurred predominately above the extrapolation of the λ line into the metastable region. This is contrary to expectations, and one would have to hypothesize a large change in the slope of the λ line or the existence of small volumes of superfluid above the λ transition to support quantized vortex production.

By analogy with the sharp peak in the heat capacity

and the attenuation of first sound as the λ line is approached, it seems probable that any enhancement of the nucleation rate in this region is due to a relaxation effect associated with the spontaneous thermal fluctuations in the order parameter.⁴⁵ The exact mechanism for enhanced nucleation near the λ line, if this phenomenon exists, remains obscure.

VII. SUMMARY AND CONCLUSION

Since helium remains liquid at low pressures to 0 K, it constitutes in many ways the ideal liquid in which to investigate the limits of tensile strength. Because it is unlikely that all sources of heterogeneous nucleation can be completely eliminated, tensile strength experiments must quickly reach deeply into the metastable region where the resulting high rate of homogeneous nucleation will mask any contribution of heterogeneous nucleation. We have carried this out using a hemispherical focusing ultrasonic transducer with laser light diffraction to detect the onset of nucleation.

Within experimental error, the tensile strength measurements were consistent with the theoretical homogeneous nucleation rate of the order of $J = 10^{15}$ critical-size nuclei/s cm^3 . As was shown in an earlier paper,²⁶ most liquids follow a law of corresponding states for homogeneous nucleation if the nucleation curves are plotted in reduced coordinates P/P_c and T/T_c , where P_c and T_c are the critical pressure and temperature. In this work, we have extended the experimental verification of nucleation theory to a reduced temperature $T/T_c = 0.3$ and a reduced pressure $P/P_c = -3.5$. This latter

represents an extension of tensile strength measurements into the negative-pressure region approximately eight times further than previously reported for any other liquid.

Finally, we would like to point out the possibility of an interesting critical anomaly. Although the data scatter is considerable, there appears to be a suggestion of a slight lowering of the magnitude of the tensile strength near the extension of the metastable λ line into the negative-pressure region. Lending some credence to this possibility is the systematic agreement in the tensile strength reduction as measured independently by both diffracted light and the acoustic power radiated. This apparent anomaly is inconsistent with the homogeneous nucleation theory based on Eqs. (6) and (8). It is perhaps unreasonable to expect a theory which does not take cognizance of the presence of a continuous phase transition (except through the liquid density and the surface tension) to be generally valid as the transition is approached. However, further measurements would be required to clarify whether this interesting tensile strength anomaly does indeed exist.

ACKNOWLEDGMENTS

This work was supported in part by National Science Foundation Grant No. DMR-8304249, and by the Environmental Sciences and Resources program at Portland State University (ESR Publication 240). We would like to acknowledge useful discussions with Dipen N. Sinha, and to thank Rudi Zupan for his technical assistance.

*Present address: Applied Superconductivity Center, University of Wisconsin, Madison, WI 53706.

¹R. E. Apfel, *J. Acoust. Soc. Am.* **49**, 145 (1971).

²J. A. Nissen, E. Bodegom, L. C. Brodie, and J. S. Semura, *Adv. Cryog. Eng.* **33**, 999 (1988).

³D. N. Sinha, Ph.D. dissertation, Portland State University (University Microfilms, Ann Arbor, MI 1980).

⁴J. E. Anderson, in *Space Cryogenics Workshop* (1988) (unpublished).

⁵J. W. Beams, *Phys. Rev.* **104**, 880 (1956).

⁶J. W. Beams, *Phys. Fluids* **2**, 1 (1959).

⁷R. C. A. Brown, H. J. Hilke, and A. H. Rogers, *Nature* **220**, 1177 (1968).

⁸H. C. Dhingra and R. D. Finch, *J. Acoust. Soc. Am.* **59**, 19 (1976).

⁹M. H. Edwards, R. M. Cleary, and W. M. Fairbank, *Quantum Fluids* (North-Holland, Amsterdam, 1966), p. 140.

¹⁰R. D. Finch, R. Kagiwada, M. Barmatz, and I. Rudnick, *Phys. Rev. A* **134**, 1425 (1964).

¹¹R. D. Finch and T. G. Wang, *J. Acoust. Soc. Am.* **39**, 511 (1966).

¹²R. D. Finch, T. G. Wang, R. Kagiwada, M. Barmatz, and I. Rudnick, *J. Acoust. Soc. Am.* **40**, 211 (1966).

¹³R. D. Finch and M. L. Chu, Jr., *Phys. Rev.* **161**, 202 (1967).

¹⁴P. D. Jarman and K. J. Taylor, *J. Low Temp. Phys.* **2**, 389 (1970).

¹⁵P. L. Marston, *J. Low Temp. Phys.* **25**, 383 (1976).

¹⁶C. F. Mate and K. L. McCloud, in *Proceedings of the Eleventh International Conference on Low Temperature Physics, St. Andrews, 1968*, edited by J. F. Allen, D. M. Einlayson, and D. M. McCall (University of St. Andrews Press, 1968), p. 308.

¹⁷P. M. McConnell, M. L. Chu, Jr., and R. D. Finch, *Phys. Rev. A* **1**, 411 (1970).

¹⁸A. D. Misener and G. R. Herbert, *Nature* **177**, 946 (1956).

¹⁹A. Mosse, M. L. Chu, Jr., and R. D. Finch, *J. Acoust. Soc. Am.* **47**, 1258 (1970).

²⁰A. Mosse and R. D. Finch, *J. Acoust. Soc. Am.* **49**, 156 (1971).

²¹E. A. Neppiras and R. D. Finch, *J. Acoust. Soc. Am.* **52**, 335 (1972).

²²J. R. Shadley and R. D. Finch, *Phys. Rev. A* **3**, 780 (1971).

²³M. F. Wilson, D. O. Edwards, and J. T. Tough, *Bull. Am. Phys. Soc.* **12**, 96 (1967).

²⁴I. Thormählen, in *Proceedings of the Eighth International Heat Transfer Conference, San Francisco, 1986*, edited by C. L. Tien, V. P. Carey, and J. K. Ferrell (Hemisphere, Washington, 1986), p. 2001.

²⁵V. A. Skripov, *Metastable Liquids* (Wiley, New York, 1974), Chaps. 1–7, pp. 1–191.

²⁶D. N. Sinha, J. S. Semura, and L. C. Brodie, *Phys. Rev. A* **26**, 1048 (1982).

²⁷K. Nishigaki and Y. Saji, *Phys. Rev. B* **33**, 1657 (1986).

²⁸D. Lezak, L. C. Brodie, J. S. Semura, and E. Bodegom, *Phys. Rev. B* **37**, 37 (1988).

²⁹J. Sapriel, *Acousto-Optics* (Wiley, New York, 1976), Chap. VI,

- pp. 54–60.
- ³⁰J. D. Jackson, *Classical Electrodynamics*, 2nd ed. (Wiley, New York, 1975), Chap. 9, p. 411.
- ³¹V. A. Akulichev, *Ultrasonics* **26**, 8 (1986).
- ³²J. A. Nissen, Ph.D. dissertation, Portland State University (University Microfilms, Ann Arbor, MI 1988).
- ³³J. A. Nissen, E. Bodegom, L. C. Brodie, and J. S. Semura (unpublished).
- ³⁴M. O'Donnell, L. J. Busse, and J. G. Miller, *Methods of Experimental Physics* **19**, (Academic, New York, 1981), p. 29.
- ³⁵K. A. Naugol'nykh and E. V. Romanenko, *Akust. Zh.* **5**, 191 (1959) [*Sov. Phys.—Acoust.* **5**, 191 (1959)].
- ³⁶E. Bodegom, J. A. Nissen, L. C. Brodie, and J. S. Semura, *Adv. Cryog. Eng.* **33**, 349 (1988).
- ³⁷L. D. Rozenberg, *High-Intensity Ultrasonic Fields* (Plenum, New York, 1971), pp. 5–71.
- ³⁸H. A. Kashkooli, P. J. Dolan, Jr., and C. W. Smith, *J. Acoust. Soc. Am.* **82**, 2086 (1987).
- ³⁹R. Becker and W. Döring, *Ann. Phys. (N.Y.)* **24**, 719 (1935).
- ⁴⁰M. Blander, and J. L. Katz, *J. Am. Inst. Chem. Eng.* **21**, 833 (1975).
- ⁴¹M. Iino, M. Suzuki, and A. J. Ikushima, *J. Low. Temp. Phys.* **61**, 155 (1985).
- ⁴²V. A. Akulichev and V. A. Bulanov, *Akust. Zh.* **20**, 817 (1974) [*Sov. Phys.—Acoust.* **20**, 501 (1975)].
- ⁴³I. M. Lifshitz and Yu. Kagan, *Zh. Eksp. Teor. Fiz.* **62**, 385 (1972) [*Sov. Phys.—JETP* **35**, 206 (1972)].
- ⁴⁴C. W. Smith and M. J. Tejwani, *Physica* **7D**, 85 (1983).
- ⁴⁵P. C. Hohnenberg, in *Proceedings of the International School of the Physics of Critical Phenomena, Varenna, 1970*, edited by M. S. Green (Academic, New York, 1971), p. 285.